RSC Advances

PAPER

View Article Online
View Journal | View Issue

Cite this: *RSC Adv.*, 2019, **9**, 12300

Adsorption–desorption behavior of the hydrophobically associating copolymer AM/APEG/C-18/SSS

Hongping Quan,[ab] Qiangying Lu,[ab] Zhonghao Chen,[ab] Zhiyu Huang*[ab] and Qingying Jiang[ab]

Received 13th March 2019
Accepted 29th March 2019

DOI: 10.1039/c9ra01932d

rsc.li/rsc-advances

In this study, acrylamide (AM), allyl polyethylene-1000 (APEG), octadecyl dimethyl allyl ammonium chloride (DMDAAC-18), and sodium styrene sulfonate (SSS) were chosen to synthesize a quadripolymer (HPAAT) in which a hydrophobic association exists between the molecules. The critical concentration of the hydrophobic association was determined using fluorescence spectrophotometry. Furthermore, HPAAT formed films by adsorbing onto a carbonate rock surface. The molecular structure of HPAAT was characterized using Fourier-transform infrared spectroscopy and ^{1}H-NMR spectroscopy, the results showed that the obtained product was consistent with the target product. The intrinsic viscosity was determined using an Ubbelohde viscometer. The molecular weight and dispersion exponent of HPAAT were determined using gel permeation chromatography. Addition of HPAAT into 20% HCl decreased the reaction rate of the acid rock obviously, even at a low viscosity. Variation of the reaction rate with time with different amounts of HPAAT was investigated using the volume of carbon dioxide gas produced. The adsorption and desorption of HPAAT on a carbonate rock surface were demonstrated using infrared spectroscopy analysis, scanning electron microscopy and ultraviolet spectrophotometry.

1 Introduction

Acidification is the main means of increasing oil and gas production. The injected acid fully covers the entire layer to be processed, and this is the key to the success of the acidification operation. However, when the acid solution is injected into the stratum, the fast reaction rate between the hydrochloric acid and carbonates means that the acid cannot penetrate into the deepest places in the carbonate reservoir. Priority is given to the formation of fractures with high permeability, while a layer with low permeability cannot be treated. The reason for the low permeability of the reservoir could be due to two reasons: one is that the reservoir is a naturally low permeability reservoir (II reservoir); the second is that the permeability of oil reservoirs are reduced owing to the pollution close to the well in the process of oil and gas development.[1–4] These unprocessed segments mean that production will be reduced and a certain amount of the reserves will be lost. Therefore, retarded acid technology is applied to give deep acidification in order to improve the effect of acid treatment, see Fig. 1.[5–9]

There are two ways to increase the retardation rate: one is to reduce the diffusion rate of the hydrogen ions by increasing the viscosity of acids.[6] and the other is to separate the acid solution from the rock by forming a film on the rock surface, thus reducing the reaction rate between the acid and the rock.[10] Recently, gelled acids have effectively improved the permeability of reservoirs as retarded acids have attracted the interest of many researchers. A gelled acid is usually composed of HCl as the base–acid and a polymer gelling agent as an addictive. The gelled acid reduces the diffusion rate of H^+ to the rock surface owing to its high viscosity and reduced filtration. However, it is difficult to penetrate into the deeper positions in the reservoir and flow back owing to the high viscosity. In this study, the acid rock reaction was slowed down mainly by forming a film on the surface of the rock.

Polymers are widely used, to date, various polymers have been successfully fabricated into nanofibrous membranes *via* electrospinning and have been evaluated for air filtration.[11] Polymeric materials have contributed significantly to the development and improvement of medical devices and systems. Novel designed polymers using ion-beam modification methods have been studied to improve blood and tissue compatibility.[12] The hydrophobic associative polymer can form a network structure by intermolecule association in a dilute solution at a certain concentration, which can cause an increase in the elastic and viscous modulus of the polymer acid solution and helps to slow down the reaction between the acid and the rock.[13–20] In oilfield

[a]*College of Chemistry and Chemical Engineering, Southwest Petroleum University, Chengdu 610500, PR China*
[b]*Oil & Gas Field Applied Chemistry Key Laboratory of Sichuan Province, Chengdu 610500, PR China*

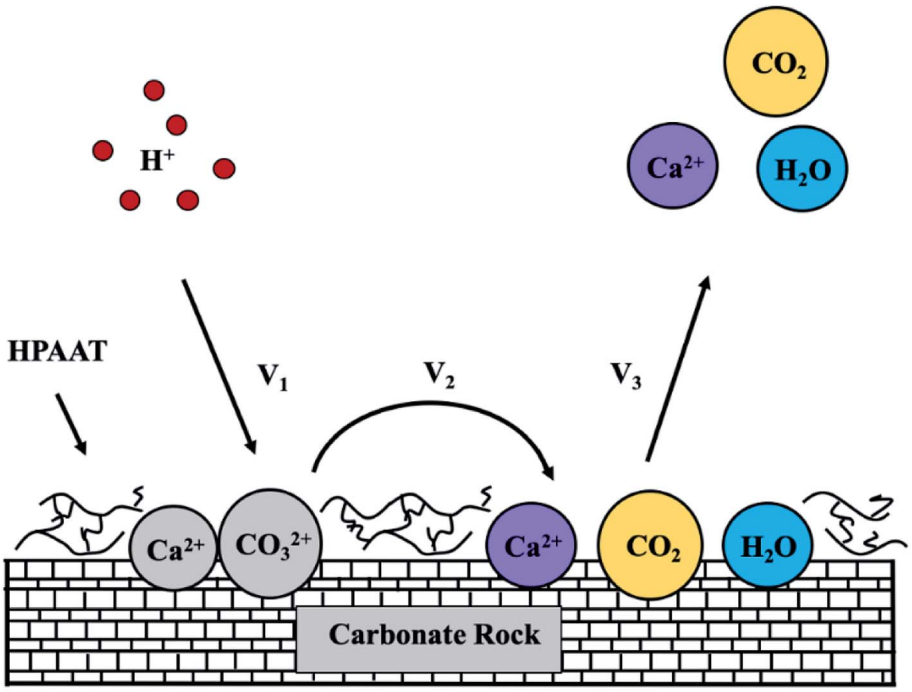

Fig. 1 Mechanistic diagram of the acid rock reaction.

applications, the hydrophobic associating polymer is adsorbed on the reservoir to allow the interaction of the polymer and the reservoir, which may have some beneficial effects on the reservoir.[21] The ability of the hydrophobic associative polymer adsorbed onto rock surfaces has attracted the attention of many researchers. However, research into the adsorption behavior of hydrophobic associative polymers and the adsorption capacity and adsorption rate have not been fully explored.[22–24]

Owing to the aforementioned problems, it is particularly important to study retarded acids that have a low viscosity and good adsorption. In our study, acrylamide (AM), allyl polyethylene-1000 (APEG), octadecyl dimethyl allyl ammonium chloride (DMDAAC-18), and sodium styrene sulfonate (SSS) were chosen to synthesize a type of hydrophobic association polymer (HPAAT), the copolymer could form a thin film by adsorbing on the rock when used as a retarded additive. The aim of the study was to research the adsorption and desorption behavior in the acid rock reaction, including the effect of the addition of the polymer.

2 Experimental

2.1 Materials

The AM, SSS, anhydrous ethanol, calcium carbonate (teaching reagent) and hydrochloric acid were obtained from Kelong, Chengdu, China and were all analytical-reagent grade chemicals. APEG-1000 was purchased from the Haian petrochemical plant, Jiangsu, China. The DMAAC-18 was of an industrial grade and was obtained from Jiangsu Fumiao Chemical Reagent Factory (China). Azodiisobutyronitrile hydrochloride (V50) was purchased from the Ipres Technology Company (China).

2.2 Synthesis

First, DMAAC-18 (0.56 g) was dissolved in 22.12 g of distilled water in a three-necked flask, and then AM (6.82 g), APEG-1000 (2.0 g) and SSS (0.103 g) were added into the solution, the solution was stirred until these were completely dissolved. Next, the initiator V50 (0.0113 g) was added into the solution, and was reacted for 5 h at 50 °C. Finally, the product was cut up and washed several times with ethanol. After washing, the product was dried at 50 °C to a constant weight, and the polymer was obtained. The molecular structure of HPAAT is shown in Scheme 1.

2.3 Characterization and experimental measurements

2.3.1 Infrared spectroscopic analysis. The pellet samples were prepared by pressing the mixture of the copolymer and KBr powder, these were then characterized using Fourier transform infrared spectroscopy (FTIR) (WQF-520, China) in the range between 4000 and 500 cm^{-1}.

2.3.2 ^{1}H-NMR spectroscopy. HPAAT was dissolved in D_2O and the structural characterization of HPAAT was performed using ^{1}H-NMR (Ascend 400 MHz, Switzerland).

2.3.3 Gel permeation chromatography. The molecular weight of HPAAT was measured using gel permeation chromatography (GPC). Samples (5 mg) were dissolved in a mixture of 1 mL acetonitrile and water (AN, H_2O volume ratio 3.5 : 6.5, using the same mobile phase), and filtered using a 0.45 μm filter membrane. These measurements were performed at room temperature (23 °C) for 90 min.

2.3.4 Determination of intrinsic viscosity. First, 0.05 g of the dried and pulverized HPAAT powder was weighed into

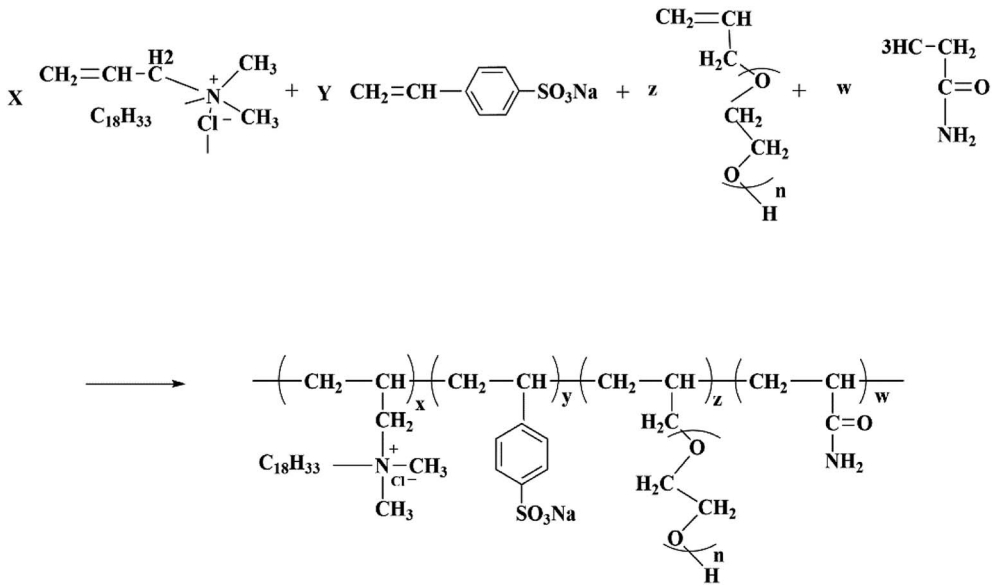

Scheme 1 Molecular structure of HPAAT.

a beaker, and then dissolved by adding a small amount of 1 mol L^{-1} sodium chloride solution. Then, the fully dissolved polymer solution was diluted into a 50 mL volumetric flask, and placed in a 1 g L^{-1} slow-adjusting admixture solution for later use. Next, a constant temperature water bath was set to 30 ± 0.05 °C. The time taken for the configured sodium chloride solution to flow through the Ubbelohde viscometer was determined, this was measured three times in parallel, and the average value was recorded as t_0. The time taken for the HPAAT solution to flow through the Ubbelohde viscometer was measured. Finally, the solution was gradually diluted with the configured sodium chloride solution (relative concentration, c), and the time taken to flow through the Ubbelohde viscometer was measured.[25]

2.3.5 Fluorescence spectrophotometry. Pyrene was weighed (30.3 mg), dissolved in methanol, transferred to a 150 mL clean volumetric flask, diluted with methanol to the scale, and prepared into a methanol solution of 1 mmol L^{-1} pyrene. The pyrene stock solution (0.04 mL, 1×10^{-3} mol L^{-1} in ethanol) was pipetted into a clean 5 mL volumetric flask with a micro sampler and the methanol was dried using nitrogen, after the ethanol had been dried, the required amount of HPAAT and 20% HCl were dissolved in a volumetric flask and subjected to ultrasound for 0.5 h.[26]

The HPAAT acid was placed at room temperature for 36 h as a backup. A fluorescence spectrophotometer was used to scan the pyrene solution. The strength of the first shock peak (373 nm) of the pyrene solution is represented as I_1, and I_3 represents the strength of the third shock peak (384 nm). The fluorescence test conditions used were: a fluorescence excitation wavelength of 335 nm, the excitation and emission slits were both 2.5 nm, the scanning range used was 350–550 nm, the scanning speed was 240 nm min^{-1}, and the voltage was 700 V.

2.3.6 Environmental scanning electron microscopy. The surface morphology and the volume changes of the carbonate were observed using environmental scanning electron microscopy (SEM, JSM7500F, Japan) at ambient temperature. The pictures were obtained at an amplification of 5000 times their real size.

2.3.7 Ultraviolet-visible spectroscopy. The polymer content in the acid solution was detected by the colorimetric method using ultraviolet-visible spectroscopy (UV-vis, PerkinElmer LS55, USA) with wavelengths of 0 to 400 nm.

2.3.8 Determination of the retarding rate. First, the marble was cut into cubes of 20 × 20 × 20 mm, then the surface area of the marble rock sample was calculated. The samples were dried in an oven and the mass was weighed. Next, a volume of 20% hydrochloric acid was placed into a beaker according to the rock sample, per unit surface area this corresponded to 20 mL hydrochloric acid. The calculated amount of the polymer powder was added into the solution and stirred until it was completely dissolved. Finally, the marble rock sample was put into the acid solution and reacted for 10 min at 75 °C, then the remaining marble rock sample was taken out quickly, rinsed and put into the oven to dry before being weighed.

The blank experiment was performed in the same way as the above described evaluation method. The carbonate sample is shown in Fig. 2 and the calculation formula of retarding rate is as follows.

$$\Delta m = m_1 - m_2 \quad (1)$$

In which, Δm is the dissolution mass of the rock sample (g), m_1 is the mass of the rock sample before the reaction (g), and m_2 is the mass of the rock sample after the reaction (g).

$$V_a = \Delta m \times 1000/(S \times \Delta t) \quad (2)$$

$$K = \frac{V_a - V_0}{V_a} \times 100\% \quad (3)$$

In which K is the retarding rate (%), V_0 is the reaction rate of the HPAAT acid and the rock (mg $(cm^2\ s^{-1})^{-1}$), and V_a is the

Fig. 2 Square sample of carbonate.

reaction rate of the blank hydrochloric acid and the rock, (mg $(cm^2\ s^{-1})^{-1}$).

2.3.9 Reaction rate of HPAAT. The calcium carbonate rocks were encased in epoxy resin, leaving only one side exposed for which the area (S) was 5 cm^2. The CO_2 gas produced by the reaction of the polymer acid solution and the calcium carbonate rocks was collected using a CO_2 gas-collecting device.[10] The acid–rock reaction rate was calculated using the volume of the collected CO_2.[27–29] The formula used is as follows:

$$u = \frac{n_{(CaCO_3)} \times M_{(CaCO_3)}}{s \times t} = \frac{n_2 \times M_{(CaCO_3)}}{s \times t} = \frac{\frac{V_2}{1000V_1} \times M_{(CaCO_3)}}{s \times t} = \frac{0.00409V_2}{s \times t} \quad (5)$$

In which, u is the reaction rate of the HPAAT acid and the carbonate rock (g cm^{-2} min^{-1}), $n_{(CaCO_3)}$ is the amount of $CaCO_3$ in mol, $M_{(CaCO_3)}$ is the molar mass of $CaCO_3$ in g mol^{-1}, n_2 is the amount of substance of CO_2 in mol, V_2 is the volume of CO_2 gas per unit of reaction time (mL), V_1 is the molar volume at 25 °C, S is 5 cm^2, and t is the reaction time (min).

3 Results and discussion

3.1 Characterization of the polymer

It can be seen from Fig. 3 that the characteristic absorption bands at 1715 cm^{-1} and 3448 cm^{-1} can be assigned to the C=O and N–H stretching vibrations of the amide groups of AM. The peaks of the benzene ring at 778 cm^{-1} and S=O at 1414 cm^{-1} confirm the existence of SSS. The peaks at 2920 and 2855 cm^{-1} are ascribed to $-CH_3$ and $-CH_2-$. The peak at 3208 cm^{-1} is the stretching vibration peak of O–H. The peaks at 1454 cm^{-1} are due to the stretching vibrations of the C–H. The peak at 1128 cm^{-1} illustrates that the C–O–C stretching vibrations from APEG exist in HPAAT. Furthermore, 1311 cm^{-1} is the stretching vibration peak of the C–N. This result is consistent with the molecular design structure.

Fig. 4 shows the ^{1}H-NMR (400 MHz, D_2O) diagram of HPAAT, in which the chemical shift of the hydrogen spectrum of HPAAT is as follows: 1.09(m, $-CH_3$), 1.25–1.36 (c, $-(CH_2)_{15}-$), 1.62 (r, l, g, $-CH_2-CH-C-O-NH_2$, $-CH_2-CH-CH_2-$, $-CH_2-CH-C$), 1.71 (q, $-N-CH_2-CH_2-$), 2.14 (n, b, $-CH-CH_2-O-$, $-CH-CH_2-N$), 2.26 (s, $-CH-C-O-NH_2$), 3.22 (z, x, $-n-CH_2-$, CH_2-N-), 3.30 (j, $-N-CH_3$), 3.63 (k, $-CH_2-O-$, $-CH_2-CH_2-O-$), 7.21 (t, $-NH_2$), 7.67 (h, –CH–CH–C). The results of the ^{1}H-NMR analysis were combined with the FTIR spectra shown in Fig. 3, we concluded that the obtained product was basically consistent with the designed molecule, which has been synthesized successfully.

The GPC data for HPAAT are shown in Table 1.

The results showed that the average weight of the polymer was lower.

As can be seen from Table 2, the intrinsic viscosity of the retarded acid was 114.65 mL g^{-1}. The intrinsic viscosity was determined using a Ubbelohde viscometer and the viscosity curve for HPAAT is shown in Fig. 5.

3.2 Critical concentration point of the hydrophobic association

As can be seen from Table 3, the reduced viscosity of the polymer acid solution is consistent with the results of the GPC tested previously. When the concentration increased from 0.7 to

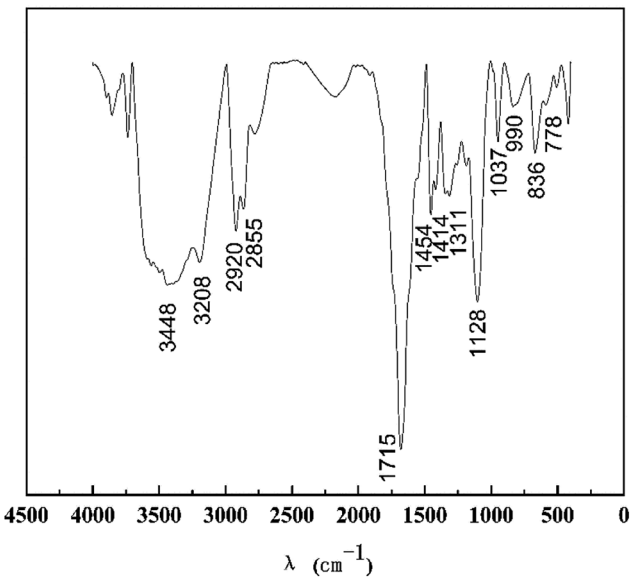

Fig. 3 FTIR spectrum of HPAAT.

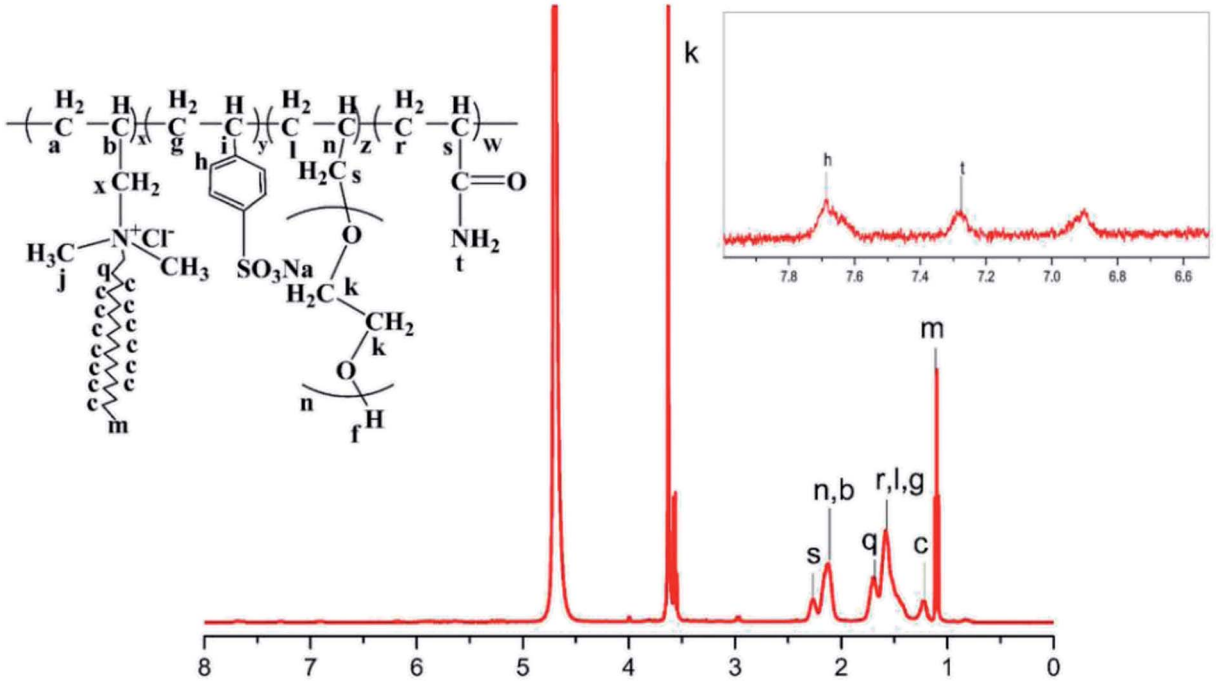

Fig. 4 Nuclear magnetic resonance spectrum of HPAAT.

0.8 wt%, the initial viscosity showed a significant increase that was determined by the apparent viscosity. The sudden increase in viscosity was due to the hydrophobic association, and the predominate intramolecular aggregation turned into predominately intermolecular aggregation.

The apparent viscosity can reflect the hydrophobic correlation effect on the macro level, whereas the hydrophobic association properties of the polymer at a molecular level can be revealed using fluorometry. Nonpolar pyrene can be used as a fluorescence probe to reflect the intensity of the hydrophobic association effect, as nonpolar pyrene can solubilize into the hydrophobic region. According to the ratio of the fluorescence absorption intensity at 373 nm compared to that at 384 nm (I_1/I_3), the solubility of pyrene can be concluded. The more polar the microenvironment around the pyrene probe, the higher the value of I_1/I_3. When the intramolecular aggregation turns predominately into intermolecular aggregation, the value of I_1/I_3 shows an obvious decrease.

Table 1 GPC results for HPAAT

M_n	M_w	M_P	M_z	$M_z + 1$	Polydispersity
1.0×10^5	2.7×10^5	6.8×10^4	5.4×10^5	8.3×10^5	2.62

Table 2 Intrinsic viscosity of the retarded acid

Curve	Fitting equation	Intrinsic viscosity number $[\eta]$ (mL g^{-1})
ln η_r/c	$y = -0.0014x + 0.1147$	114.65
η_{sp}/c	$y = 0.0006x + 0.1148$	

Table 3 Apparent viscosity of the polymer acid solution at different concentrations

Mass concentration (wt%)	Initial viscosity (mPa s)	Viscosity of residual acid (mPa s)
0.5	6	3
0.6	9	3
0.7	9	3
0.8	21	6
0.9	27	6

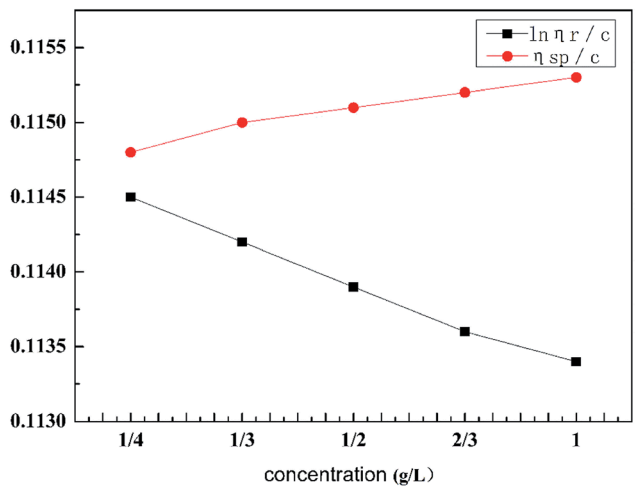

Fig. 5 Viscosity curve for HPAAT.

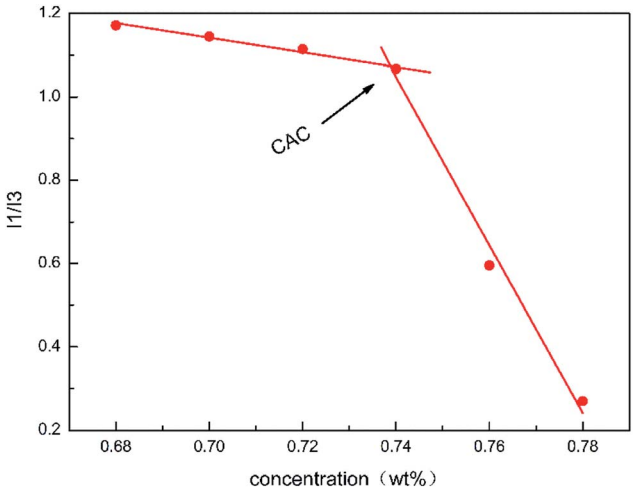

Fig. 6 Fluorescence intensity.

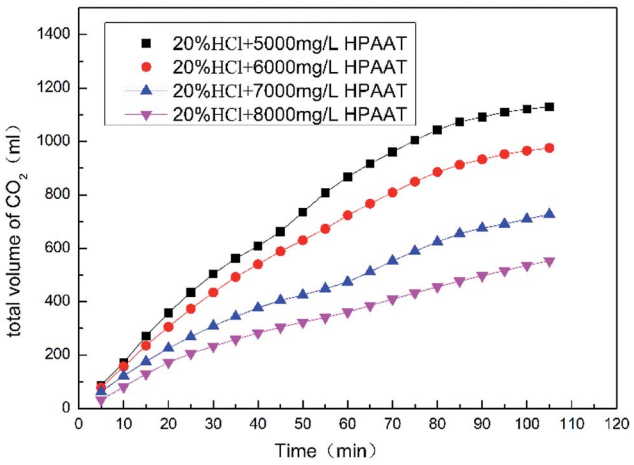

Fig. 8 Total volume of CO_2 at different concentrations of HPAAT in acid.

Fig. 6 shows the value of I_1/I_3 at different mass concentrations of the polymer acid solution. When the concentration surpassed 0.74 wt%, the value of I_1/I_3 fell abruptly, which was therefore considered to be the critical concentration of the hydrophobic association. To some extent, this is consistent with the results previously determined using the apparent viscosity. This result indicated that when the concentration of the polymer acid solution was larger than 0.74 wt% many hydrophobic areas were formed in the solution, while the polarity of the surrounding microenvironment was weakened.

3.3 Retarding capability test

It can be seen from Fig. 7 that as the concentration of HPAAT increased, the retarding rate also increased. When the concentration of HPAAT ranges from 7000 to 8000 mg L^{-1}, the increased trend in the retarding rate is basically stable, which is about 5%.

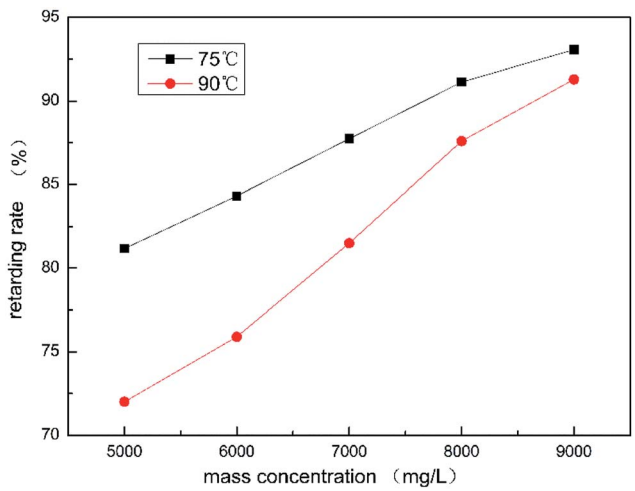

Fig. 7 Retarding rate of the HPAAT acid and carbonate at different concentrations.

In summary, it is not the hydrophobic association that effects the retarding rate of the polymer acid solution. The reason may be that the polymer adsorbs onto the carbonate surface during the acid–rock reaction.

3.4 Determination of the reaction rate

As can be seen from Fig. 8, with the increasing polymer concentration, the amount of carbon dioxide produced during the acid–rock reaction decreased. As shown in Fig. 9, as the time increased, the rate of the reaction first decreased and later increased. The results showed that the reason for the reducing reaction rate of the acid rock is because the polymer solution formed a thin film on the surface of the carbonate rock, which impeded the contact between H^+ and the surface of the carbonate rock. As the reaction continued, the reaction rate dropped to a minimum and the adsorption reached saturation. The reaction time required to reach adsorption saturation also increased as the polymer concentration increased. With the continued reaction, the polymer broke off from the rock surface, and the dissolution rate increased in an obvious manner. Finally, the reaction rate gradually decreased, mainly owing to the consumption of H^+ and the formation of a large amount of Ca^{2+}.

4 Mensuration of adsorption–desorption

4.1 UV spectrophotometric analysis of polymer solutions

The test sample was prepared by mixing 0.8 g of the polymer powder with 100 mL of 20% HCl in a conical bottom glass tube, this was then made into a polymer acid solution of 8000 mg L^{-1}, the solution underwent ultrasonic vibration for 30 min and was left to rest for 24 h. After the repose time, the test samples were prepared, the prepared solution of 8000 mg L^{-1} was diluted with 20% HCl, to obtain samples (solutions 1–8) with final concentrations from 1000 to 8000 mg L^{-1}, all samples were prepared at ambient temperature. The absorbance of the

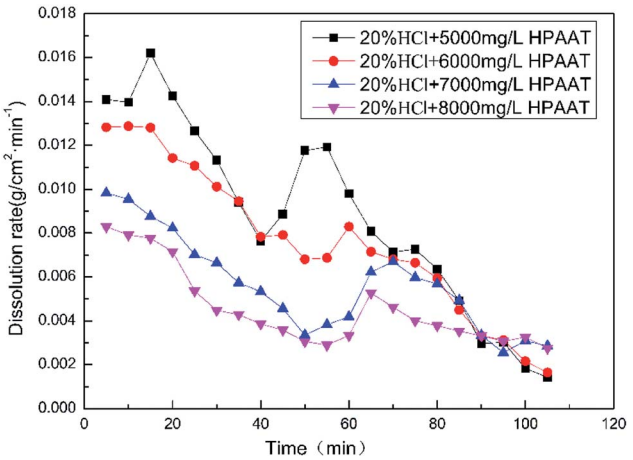

Fig. 9 Dissolution rate of HPAAT acid and the rock at different concentrations of HPAAT.

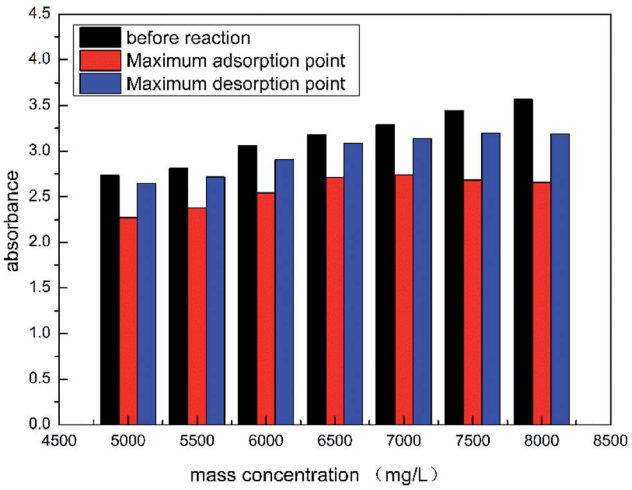

Fig. 11 UV absorbance of HPAAT acid at different concentrations.

diluted samples was obtained using 100 mm optical path quartz cells in an ultraviolet-visible spectrometer (UV-vis, PerkinElmer LS55, USA) at a selected wavelength of 233.7 nm.[30] The results are shown in Fig. 10.

The linear relationship between the absorbance and the mass concentration can be observed in Fig. 10. The corresponding HPAAT concentration can be found by the absorbance, which was detected using UV-vis spectroscopy. The absorbance at the maximum adsorption point was determined using UV-vis spectroscopy. The mass concentration was found by referring to the standard curve displayed above, thereby calculating the amount of adsorption. The polymer adsorption on the rock surface was measured using the depletion method.[31]

As shown in Fig. 11, the absorbance of HPAAT acid at the initial, maximum adsorption point and maximum desorption point can be clearly seen.

Formula for calculation of the adsorption amount:

$$Q = \frac{C_0 - C}{w} \quad (6)$$

In which, Q is the adsorption amount (mg g^{-1}), C_0 represents the initial concentration of HPAAT acid (mg L^{-1}), C is the concentration of HPAAT acid after adsorption (mg L^{-1}), and w is the carbonate concentration in the polymer-calcium carbonate dispersion (g L^{-1}).

As the fixed reaction contact is 5 cm^2 during the acid–rock reaction, the carbonate concentration in the polymer-calcium carbonate dispersion is approximately equal, therefore the amount of adsorption can be expressed by the difference in concentrations.

According to Fig. 12, as the concentration of the retarded acid increased, the difference between the concentration (absorption amount) at the maximum adsorption point and before the reaction gradually increased during the acid–rock reaction. Therefore, the higher the concentration of the retarded acid, the greater the amount of adsorption during the acid–rock reaction.

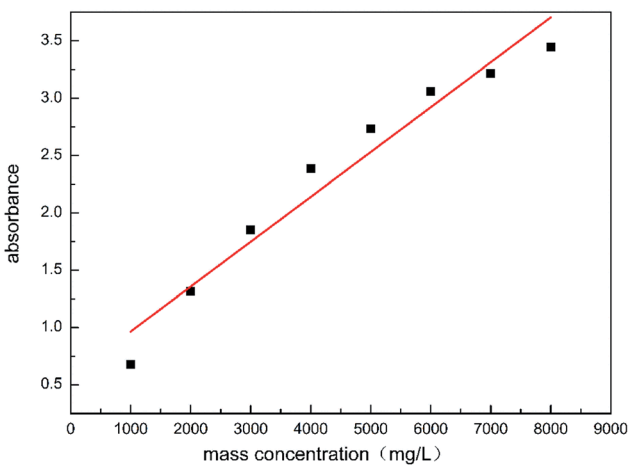

Fig. 10 Ultraviolet absorbance of samples with different concentrations.

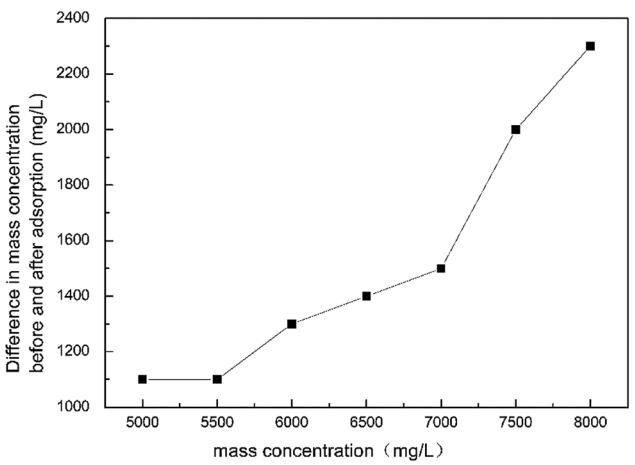

Fig. 12 Adsorption value of HPAAT acid at different concentrations.

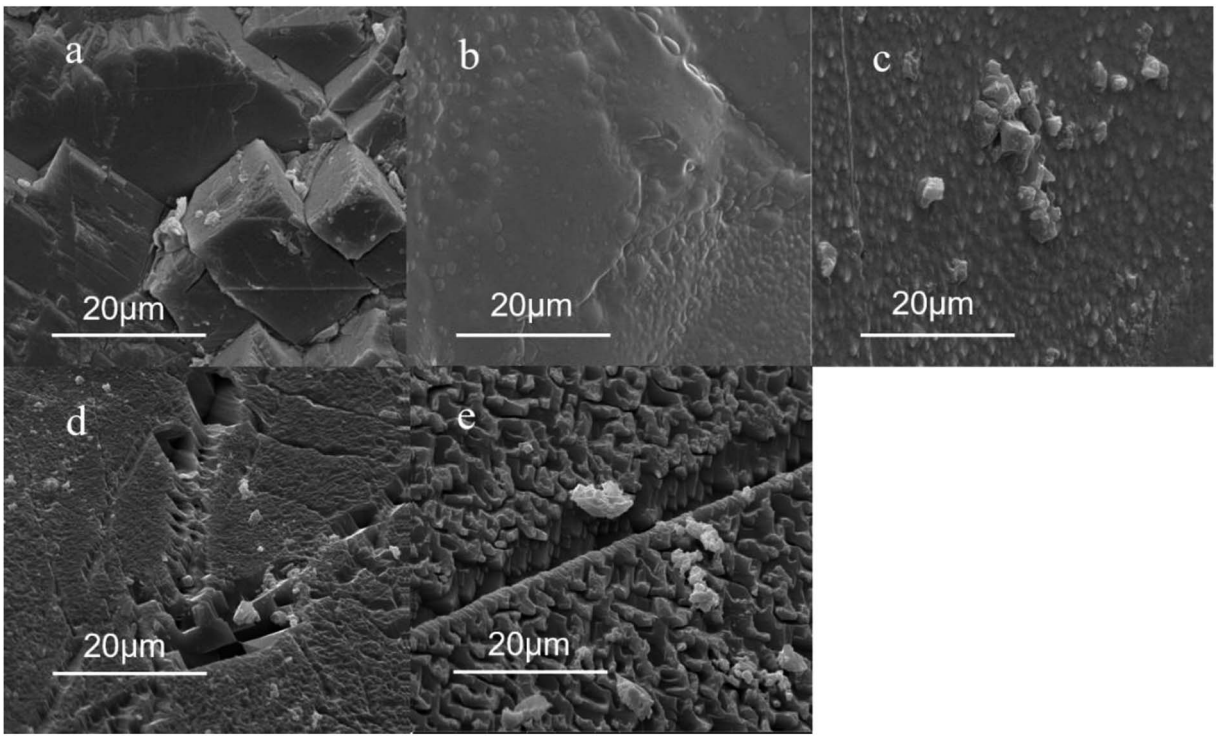

Fig. 13 Environmental SEM of samples at various dissolution times: (a) the untreated carbonate sample, (b) 5000 mg L^{-1} HPAAT-40 min (c) 8000 mg L^{-1} HPAAT-50 min, (d) 5000 mg L^{-1} HPAAT-55 min, and (e) 8000 mg L^{-1} HPAAT-65 min.

4.2 SEM analysis of the carbonate

Scanning electron microscopy was performed on the rock to explore whether the adsorption of the polymer acid solution on the rock surface is affected by hydrophobic association, as well as to investigate the micro-morphology of the rock surface before and after the adsorption of the polymer during the reaction of the acid and the rock. The results are shown in Fig. 13.

Fig. 13a shows the SEM results demonstrating the roughness of the rock surface without the acid rock reaction. As shown in Fig. 13b, a thin-layer film was formed on the carbonate sample that was treated with 20% HCl and 5000 mg L^{-1} polymer acid solution for 40 min, and the carbonate rock surface looked smooth. As shown in Fig. 13d, for the carbonate sample that was treated with the polymer acid solution for 55 min a large number of cracks and voids were formed, meanwhile the thin film broke away from the carbonate surface and only a small amount of polymer remains. By comparing Fig. 13c with Fig. 13b it can be seen that the adsorption of the polymer on the calcium carbonate surface is significantly increased. As seen in Fig. 13e the adsorption film broke away from the carbonate surface. This showed that the added polymer could be absorbed onto the carbonate rock surface, and desorbed from the carbonate, leaving a small amount of polymer on the surface of the rock, with very little damage to the rock.

4.3 Infrared spectroscopy analysis of the carbonate rock surface

In this study, the infrared spectra of the carbonate rock surface were determined using WQF-520 Fourier-transform infrared spectroscopy at various points at which the rock and the 0.5 wt% HPAAT acid reacted. The surface changes of the carbonate rock samples before and after the acid–rock reaction were verified. The results are shown in Fig. 14.

According to the infrared spectrum analysis, the carbonate rock spectrum before the reaction showed peaks at 3442.32, 2985.27, 2869.56, 2508.94, 875.52, 703.89 and 1600–1300 cm^{-1}. These broad and strong absorption peaks are the absorption vibration peaks of calcium carbonate. The marble samples were dissolved for 40 min (the maximum adsorption point of 0.5 wt%

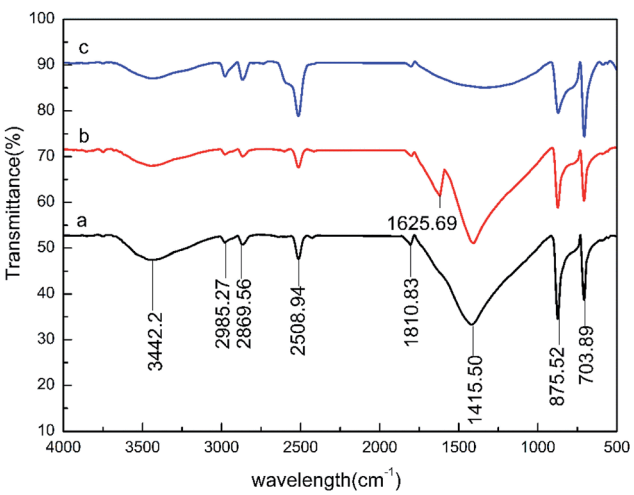

Fig. 14 Infrared spectrogram of the carbonate rock surface: (a) before reaction; (b) at the maximum adsorption point; and (c) at the maximum desorption point.

HPAAT). Compared with the absorption peaks of before the reaction (Fig. 14a) and the maximum adsorption point (Fig. 14b), the C=O stretching vibration peak of the amide group at 1625.69 cm^{-1} at the maximum adsorption point indicates that during the acid–rock reaction the HPAAT was adsorbed onto the surface of the carbonate. It can be seen from the carbonate at the maximum desorption point (Fig. 14c) compared with the carbonate rock before dissolution (Fig. 14a) that the infrared analysis spectrum of the two are consistent, and the C=O stretching vibration peak without the amide group indicates that the HPAAT has been taken off the marble surface.

5 Conclusions

In this study, a copolymer with a low viscosity and adsorption was developed to address the disadvantages of the short penetration distance, and the difficulty in injection and flowback in the process of acidification in oil and gas fields. HPAAT was obtained by free radical aqueous solution polymerization using four monomers: AM, APEG, DMAAC-18 and SSS. The initial viscosity and residual viscosity of the HPAAT were lower, which is beneficial to the injection and the flowback. The HPAAT adsorbed and formed a protective film on the carbonate, preventing the hydrogen ions from contacting the rock surface and improving the retarding effect of the acid. The molecular structure of HPAAT was characterized using FTIR and ^{1}H-NMR spectroscopy. The weight-average molecular weight (M_w) was 2.7 $\times 10^5$, the number-average molecular weight (M_n) was 1.0 $\times 10^5$, and the polydispersity was equal to 2.62. Analysis was conducted for HPAAT at the concentrations of 5, 6, 7, 8 and 9 g L^{-1} The apparent viscosity showed that HPAAT at 7 g L^{-1} has a high retarding efficiency and the viscosity of the acid remained under 10 mPa. The retarding capability test implied that the absorption of HPAAT on the surface of the carbonate rock hindered the contact between H^+ and the surface. The SEM, infrared spectrum analysis, and UV analysis implied that before and after the hydrophobic association the polymer adsorbed onto the surface of carbonate and formed a layer of adsorption film. After the acid and carbonate rock reacted, the absorption film was broken away from the surface of the carbonate, and a small amount of polymer remained on the carbonate surface and formed lots of cracks and voids. Therefore, the adsorption and desorption influenced the reaction rate of the acid and the carbonate. We plan to conduct further research on the application of the copolymer in the future.

Conflicts of interest

There are no conflicts to declare.

Acknowledgements

This work was supported by the National Natural Science Foundation of China (No. 51604229) and the Sichuan Science and Technology Plan Project (No. 2019YJ0315).

References

1 D. E. Johnson, K. B. Fox, L. D. Burns and E. M. O'Mara, *Carbonate Production Decline Rates Are Reduced through Improvements in Gelled Acid Technology*, SPE, Midland, Texas, 1988.
2 A. S. Pabley and D. L. Holcomb, *A New Method of Acidizing of Acid Fracturing: Crosslinked Acid Gel*, Annual Southwestern Petroleum Short Course, Dallas, Texas, 1980.
3 L. N. Morgenthaler, *Application of a Three-Dimensional Hydraulic Fracturing Simulator for Design of Acid Fracturing Treatments*, Society of Petroleum Engineers, Oklahoma, 1993.
4 T. D. Welton and S. V. Domelen, *High-viscosity-yield acid systems for high-temperature stimulation*, Society of Petroleum Engineers, Lafayette, Louisiana, 2006.
5 M. Steven, W. Brian, W. Davis, D. H. Gray and J. M. Brienen, *Acid Fracturing in the Warrent Unit of Southeastern New Mexico*, Society of Petroleum Engineers, Dallas, Texas, 1996.
6 G. D. Dean, C. A. Nelson, S. Metcalf, R. Harris and T. Barber, *New Acid System Minimizes Post Acid Stimulation Decline Rate in the Wilmington Field*, SPE, Bakersfield, California, 1998.
7 J. Mou, S. Zhang and Y. Zhang, Acid Leakoff Mechanism in Acid Fracturing of Naturally Fractured Carbonate Oil Reservoirs, *Transp. Porous Media*, 2012, **91**(2), 573–584.
8 M. A. Sayed, H. A. Nasr-El-Din, J. Zhou and S. A. Holt, *New Emulsified Acid to Stimulate Deep Wells in Carbonate Reservoirs*, Society of Petroleum Engineers, Cairo, Egypt, 2011.
9 P. Y. Feng, D. Wang, G. Z. Liu, H. B. Wang and M. John, *Reservoir Stimulation Using High-Temperature Deep-Penetrating Acid*, Society of Petroleum Engineers, Anchorage, Alaska, 2011.
10 H. Quan, H. Li, Z. Huang, *et al.*, Copolymer MCJS as a retarder of the acid–rock reaction speed for the stimulation of deep carbonate reservoirs, *J. Appl. Polym. Sci.*, 2015, **132**(7), 2259–2262.
11 D. Lv, R. Wang, G. Tang, *et al.*, Eco-friendly Electrospun Membranes Loaded with Visible-light Response Nanoparticles for Multifunctional usages: High-efficient Air Filtration, Dye Scavenger and Bactericide, *ACS Appl. Mater. Interfaces*, 2019, DOI: 10.1021/acsami.9b01508.
12 Y. Suzuki, Ion beam modification of polymers for the application of medical devices, *Nucl. Instrum. Methods Phys. Res., Sect. B*, 2003, **206**(03), 501–506.
13 H. A. Nasr-El-Din, A. M. Al-Othman, K. C. Taylor, *et al.*, Surface tension of HCl-based stimulation fluids at high temperatures, *J. Pet. Sci. Eng.*, 2004, **43**(1), 57–73.
14 X. Song, M. Cao, Y. Han, *et al.*, Adsorption of hydrophobically modified poly(acrylamide)-co-(acrylic acid) on an amino-functionalized surface and its response to the external solvent environment, *Langmuir*, 2007, **23**(8), 4279.
15 A. A. Rakhnyanskaya, I. D. Pebalk, V. N. Orlov, *et al.*, Controlled adsorption-desorption of cationic polymers on the surface of anionic latex particles, *Polym. Sci.*, 2010, **52**(5), 483–489.

16 K. C. Taylor, R. A. Burke, *et al.*, Development of a flow injection analysis method for the determination of acrylamide copolymers in oilfield brines, *J. Pet. Sci. Eng.*, 1998, **21**(1–2), 129–139.
17 M. Alkhaldi, Reaction of citric acid with calcite, *Chem. Eng. Sci.*, 2007, **62**(21), 5880–5896.
18 F. Civan, J. Vasquez, D. Darymple, *et al.*, Laboratory and Theoretical Evaluation of Gelation Time Data for Water-Based Polymer Systems for Water Control, *Liq. Fuels Technol.*, 2007, **25**(3), 19.
19 E. Volpert, J. Selb, F. Candau, *et al.*, Adsorption of Hydrophobically Associating Polyacrylamides on Clay, *Langmuir*, 1998, **14**(7), 1871–1874.
20 K. C. Taylor and H. A. Nasreldin, Water-soluble hydrophobically associating polymers for improved oil recovery: A literature review, *J. Pet. Sci. Eng.*, 1995, **19**(3–4), 265–280.
21 H. Quan, Z. Chen, Y. Wu, *et al.*, Adsorption behavior of the copolymer AM/DMC/APEG/DMAAC-16 on a carbonate rock and its application for acidizing, *Petrochem. Technol.*, 2017, **40**(8), 895–900.
22 P. Zhang, W. Huang, Z. Jia, *et al.*, Conformation and adsorption behavior of associative polymer for enhanced oil recovery using single molecule force spectroscopy, *J. Polym. Res.*, 2014, **21**(8), 523.
23 Y. A. Shashkina, Y. D. Zaroslov, V. A. Smirnov, *et al.*, Hydrophobic aggregation in aqueous solutions of hydrophobically modified polyacrylamide in the vicinity of overlap concentration, *Polymer*, 2003, **44**(8), 2289–2293.
24 P. Zhang, Y. Wang, W. Chen, *et al.*, Preparation and Solution Characteristics of a Novel Hydrophobically Associating Terpolymer for Enhanced Oil Recovery, *J. Solution Chem.*, 2011, **40**(3), 447–457.
25 T. Wan, C. Zou, L. Chen, *et al.*, Synthesis and Solution Properties of Hydrophobically Associative Polyacrylamides by Microemulsion Polymerization, *J. Solution Chem.*, 2014, **43**(11), 1947–1962.
26 H. Quan, Z. Li and Z. Huang, Self-assembly properties of a temperature and salt-tolerant amphoteric hydrophobically associating polyacrylamide, *RSC Adv.*, 2016, **6**(54), 49281–49288.
27 Y. Du, C. Zhou, T. Zhou, *et al.*, Preparation of acrylate oligomer and its application in the modification of waterborne polyurethane, *Petrochem. Technol.*, 2011, **40**(8), 895–900.
28 M. H. Al-Khaldi, H. A. Nasr-El-Din, S. Mehta, *et al.*, Reaction of citric acid with calcite, *Chem. Eng. Sci.*, 2007, **62**(21), 5880–5896.
29 K. Lund, H. S. Fogler, C. C. Mccune, *et al.*, Acidization—IV: Experimental correlations and techniques for the acidization of sandstone cores, *Chem. Eng. Sci.*, 1976, **31**(5), 373–380.
30 J. F. Argillier, A. Audibert, J. Lecourtier, *et al.*, Solution and adsorption properties of hydrophobically associating water-soluble polyacrylamides, *Colloids Surf., A*, 1996, **113**(3), 247–257.
31 H. Lu and Z. Huang, Solution and Adsorption Properties of Hydrophobically Associating Polyacrylamide Prepared in Inverse Microemulsion Polymerization, *J. Macromol. Sci., Part A*, 2009, **46**(4), 412–418.